Filomat 33:3 (2019), 667–682
https://doi.org/10.2298/FIL1903667A

Published by Faculty of Sciences and Mathematics,
University of Niš, Serbia
Available at: http://www.pmf.ni.ac.rs/filomat

The Numerical Solution of Fredholm-Hammerstein Integral Equations by Combining the Collocation Method and Radial Basis Functions

Pouria Assari[a]

[a]*Department of Mathematics, Faculty of Sciences, Bu-Ali Sina University, Hamedan 65178, Iran*

Abstract. Hammerstein integral equations have been arisen from mathematical models in various branches of applied sciences and engineering. This article investigates an approximate scheme to solve Fredholm-Hammerstein integral equations of the second kind. The new method uses the discrete collocation method together with radial basis functions (RBFs) constructed on scattered points as a basis. The discrete collocation method results from the numerical integration of all integrals appeared in the approach. We employ the composite Gauss-Legendre integration rule to estimate the integrals appeared in the method. Since the scheme does not need any background meshes, it can be identified as a meshless method. The algorithm of the presented scheme is interesting and easy to implement on computers. We also provide the error bound and the convergence rate of the presented method. The results of numerical experiments confirm the accuracy and efficiency of the new scheme presented in this paper and are compared with the Legendre wavelet technique.

1. Introduction

Consider the following Fredholm-Hammerstein integral equation of the second kind:

$$u(x) - \lambda \int_a^b K(x,y)\Psi(y,u(y))\mathrm{d}y = f(x), \quad a \le x, y \le b, \;\; a, b \in \mathbb{R}, \tag{1}$$

where the kernel function $K(x,y)$ and the right-hand side function $f(x)$ are given, the unknown function $u(x)$ must be determined, $\lambda \in \mathbb{R}$ is a non-zero constant and the known function Ψ is continuous and nonlinear respect to the variable u. Many problems of mathematical physics, engineering and mechanics can be stated in the form of Hammerstein integral equations [24, 42, 44]. These types of integral equations also deduce from a reformulation of boundary value problems with a certain nonlinear boundary condition [13, 14, 21].

Several methods based on the basic functions so-called projection methods including collocation and Galerkin methods have been given for these types of integral equations. The discrete collocation method [11], the new collocation-type method [38, 39], the iterated Galerkin methods [37], the discrete Galerkin method [12] and the modified iterated projection method [28] have been applied to solve nonlinear Hammerstein integral equations. The Nystrom method with the existence of asymptotic error expansion [9, 31],

2010 *Mathematics Subject Classification*. 45G99; 65G99; 47H30
Keywords. Hammerstein integral equation, Discrete collocation method, Radial basis function, Meshless method, Error analysis
Received: 30 June 2017; Accepted: 06 September 2018
Communicated by Marko Petković
Email address: passari@basu.ac.ir (Pouria Assari)

the Walsh-Hybrid function approach [46], the Adomian decomposition scheme [54] and the discrete Legendre spectral method [16] have been described the numerical solution of nonlinear integral equations of the second kind. Furthermore, Haar wavelets [40], rationalized Haar wavelets [22], Legendre wavelets [1, 36] have been investigated for solving Hammerstein integral equations.

The RBFs are effective techniques for interpolating an unknown function on a scattered set of points which have been used in the past few decades. These functions involve a single independent variable regardless of the dimension of the problem, so applying them in higher dimensions does not increase the difficulties. It should be mentioned that the RBF method does not require any domain elements, so it is meshless. Firstly, Hardy [32] has studied RBFs as a multidimensional scattered interpolation method in the modeling of the earth's gravitational field in 1971 called multiquadrics and inverse multiquadrics. The thin plate splines as a type of free shape parameter RBFs have been developed by Meinguet [43] and investigated for smoothing noisy multidimensional data by Wahba [50]. Franke [27] has published a review paper in the comparison of scattered data approximations available in early 1980.

In recent years, the implication of RBFs has been shifted from scattered data interpolation to the numerical solution of partial differential equations (PDEs). RBF method has been developed for solving various types of PDEs such as the one-dimensional nonlinear Burgers equation with shock wave [33], shallow water equations for tide and currents simulation [34], heat transfer problems [56], parabolic equation with nonlocal boundary conditions [49], financial mathematics problems [35], KdV equation [18], Klein-Gordon equation [20], improved Boussinesq equation [48], sine-Gordon equation [19] and inverse wave propagation problems [51]. The author of [52] has presented comparisons on the performances among five typical RBFs for solving problems arising from engineering industries and applied sciences. Also, the useful research work [53] has studied the subdomain RBF collocation method for solving fracture mechanics problems.

We would like to review some of the most recent works for the numerical solution of integral equations utilizing the meshless methods. The meshless discrete collocation schemes have been investigated using RBFs for solving Fredholm integral equations on non-rectangular domains with sufficiently smooth kernels [2] and weakly singular kernels [6, 7]. The meshless product integration (MPI) method [5] has been proposed to solve one-dimensional linear weakly singular integral equations. The moving least squares (MLS) collocation method has been used for solving linear and nonlinear two-dimensional integral equations on non-rectangular domains [4, 45] and integro-differential equations [17]. A local meshless Galerkin method [3] has been utilized to solve weakly singular linear integral equations of the second kind. An MLS-based scheme has been applied for the numerical solution of boundary integral equations [8, 41].

In this paper, we present a method for obtaining the numerical solution of the second-kind Hammerstein integral equation (1). The method estimates the solution using the collocation method based on the use of RBF approach. The numerical scheme developed in the current paper utilizes the Gauss-Legendre quadrature rule for approximating integrals. We study the error analysis of the proposed method and demonstrate that the convergence rate of the approach is arbitrarily high. The new technique is tested over several Hammerstein integral equations and obtained results confirm the theoretical error estimates. In the following, we list some advantages of the proposed method for solving Hammerstein integral equations:

✓ The method is meshless, since it requires no domain elements.
✓ The new algorithm is simple and computationally attractive.
✓ The technique obtains more accurate results using fewer bases in compared with other methods.
✓ The iteration methods for solving the nonlinear final system corresponding to the method have less compactions.
✓ The scheme does not increase the difficulties for higher dimensional problems due to the easy adaption of RBF.
✓ The approach is more flexible for most classes of Hammerstein integral equations.

The outline of the paper is as follows: In Section 2, we present a computational method for solving Fredholm-Hammerstein integral equations of the second kind (1) utilizing the RBF scheme. In Section 3, we provide the error analysis for the new method. Numerical examples are given in Section 4. Finally, we conclude the article in Section 5.

2. RBF Collocation method

In this section, the RBF collocation method is applied for solving the Fredholm-Hammerstein integral equation of the second kind (1). We introduce the operators $\mathcal{K}$ and $\mathcal{R}$ on $C[a,b]$ as

$$\mathcal{K}u(x) = \int_a^b K(x,y)u(y)\mathrm{d}y, \quad a \le x, y \le b, \tag{2}$$

and

$$\mathcal{R}u(x) = \Psi(x,u(x)), \quad a \le x \le b. \tag{3}$$

We suppose that the function Ψ satisfies the following assumptions [37, 38]:

A1. There exists $C_1 > 0$ such that

$$|\Psi(x,u_1) - \Psi(x,u_2)| \le C_1|u_1 - u_2|, \quad \text{for all } u_1, u_2 \in \mathbb{R}.$$

A2. There is a constant $C_2 > 0$ such that $\frac{\partial\Psi}{\partial u}$ confirms

$$|\frac{\partial\Psi}{\partial u}(x,u_1) - \frac{\partial\Psi}{\partial u}(x,u_2)| \le C_2|u_1 - u_2|, \quad \text{for all } u_1, u_2 \in \mathbb{R}.$$

A3. $\Psi(.,u(.))$, $\frac{\partial\Psi}{\partial u}(.,u(.)) \in C[a,b]$ for $u(x) \in C[a,b]$.

Therefore the integral equation (1) can be represented in operator form as

$$(I - \lambda\mathcal{K}\mathcal{R})u = f. \tag{4}$$

Let $\{x_1, ..., x_N\}$ be a given set of distinct nodal points selected arbitrarily in the interval $[a,b]$. To approximate a function $u(x)$ using the radial function $\Phi(x) = \phi(|x|)$, we can give the following linear combination [55]:

$$u(x) \approx \sum_{k=1}^{N} \bar{c}_k \phi(|x - x_k|), \quad x \in [a,b]. \tag{5}$$

In this paper, we use two well-known RBFs introduced as [55]

1. The Gaussians

$$\Phi(x) = e^{(-c|x|^2)}, \ c > 0.$$

2. The inverse multiquadrics

$$\Phi(x) = (|x|^2 + c^2)^{-1/2}, \ c > 0.$$

The Gaussian and inverse multiquadrics are strictly positive definite functions on $\mathbb{R}$ [25]. This property guarantees that the associated interpolation matrixes based on them are non-singular [55] although is ill-conditioned. In most cases, the accuracy of the RBF solution depends heavily on the choice of a parameter c known as the shape parameter [55]. Many authors have investigated the shape parameter [26]. For example, in his original work on (inverse) multiquadric interpolation in $\mathbb{R}^2$ Hardy [32] suggested using $c = 0.815d$, where $d = (1/N)\sum_{i=1}^{N} d_i$, and d_i is the distance from x_i to its nearest neighbor. Later Franke [27] suggested using $c = 1.25(D/N)$, where D is the diameter of the smallest circle containing all data points. Recently, the papers [29, 30] have investigated a beneficial way of finding the optimal values of the shape parameters based on the local Taylor expansions.

The coefficients $\{\bar{c}_1, ..., \bar{c}_N\}$ in the expansion (5) are determined by solving the following system that is obtained by replacing this expansion with $u(x)$ and pick distinct node points $x_1, x_2, ..., x_N$ in the integral equation (1) as

$$\sum_{k=1}^{N} \bar{c}_k \phi(|x_i - x_k|) - \lambda \int_a^b K(x_i,y)\Psi\left(y, \sum_{k=1}^{N} \bar{c}_k \phi(|y - x_k|)\right)\mathrm{d}y = f(x_i), \quad i = 1, ..., N. \tag{6}$$

We can represent the nonlinear system (6) in the abstract form

$$\bar{u}_N = (I - \lambda \mathcal{P}_N \mathcal{K} \mathcal{R}) \bar{u}_N. \tag{7}$$

The iteration methods, such as Newton's method, for solving such cumbersome nonlinear system require to compute several definite integrals at each step of the iteration and so, they are usually sensitive to the selection of initial guess [38]. As a remedy, we recommend the following new approach based on the use of the idea in [38]. Define

$$z(x) = \Psi(x, u(x)).$$

Solve the equivalent integral equation

$$z(x) = \Psi\left(x, f(x) + \lambda \int_a^b K(x, y) z(y) \mathrm{d}y\right), \quad a \le x, y \le b, \tag{8}$$

or in the abstract form

$$z = \mathcal{R}(f + \lambda \mathcal{K} z), \tag{9}$$

for unknown $z(x)$. Then the solution of original integral equation (1) is obtained by

$$u(x) = f(x) + \lambda \int_a^b K(x, y) z(y) \mathrm{d}y, \quad a \le x, y \le b. \tag{10}$$

Therefore we can rewrite the integral equation (10) in the operator form as

$$u = f + \lambda \mathcal{K} z. \tag{11}$$

Similarly, we estimate the unknown function $z(x)$ by selecting N nodal points on the interval $[a, b]$ such as $a \le x_1 < x_2 < ... < x_N \le b$, and using the RBF ϕ as follows:

$$z(x) \approx \bar{z}_N(x) = \sum_{k=1}^{N} \bar{z}_k \phi(|x - x_k|), \quad a \le x \le b. \tag{12}$$

We replace the expansion (12) with $z(x)$ and pick distinct node points $x_1, x_2, ..., x_N$ in the integral equation (8) which conclude the following nonlinear system:

$$\sum_{k=1}^{N} \bar{z}_k \phi(|x_i - x_k|) = \Psi\left(x_i, f(x_i) + \lambda \sum_{k=1}^{N} \bar{z}_k \int_a^b K(x_i, y) \phi(|y - x_k|) \mathrm{d}y\right), \tag{13}$$

or in the operator form, we have

$$\bar{z}_N = \mathcal{R} \mathcal{P}_N (f + \lambda \mathcal{K} \bar{z}_N). \tag{14}$$

The discrete collocation methods result from the numerical integration of all integrals in the system (13). In this situation, an advantage of the method proposed in this paper is that the internal integrals on the right side of (13) need to be calculated once only, since they are dependent only on the basis (not on the unknowns) and result in a closed set of algebraic nonlinear equations for the N unknowns [38]. In the current work, we use a composite q_N-point Gauss-Legendre rule for singular integrals with M non-uniform subdivisions. Suppose that $f(x)$ is defined on (a, b) satisfies

$$|f^{(2q_N)}(x)| \le C, \tag{15}$$

for all $x \in (a, b)$. Then, for any given integer $M > 0$,

$$\int_a^b f(x) \mathrm{d}x = \frac{\Delta x}{2} \sum_{q=1}^{M} \int_{-1}^{1} f\left(\frac{\Delta x}{2} x + (q - \frac{1}{2}) \Delta x\right) \mathrm{d}x + O(\frac{1}{M^{2q_N}}), \tag{16}$$

where $\Delta x = \frac{b-a}{M}$. Now, we apply q_N-point Gauss-Legendre quadrature rule relative to the coefficients $\{\theta_k\}$ and weights $\{w_k\}$ in the interval $[-1, 1]$ to approximate integrals in (16), we obtain

$$\int_a^b f(x)\mathrm{d}x = \sum_{q=1}^{M}\sum_{k=1}^{q_N} w_k \frac{\Delta x}{2} f(\theta_k^q) + O(\frac{1}{M^{2q_N}}), \tag{17}$$

where $\theta_k^q = \frac{\Delta x}{2} v_\ell + (q - \frac{1}{2})\Delta x$. It should be noted that $\phi(|y - x_k|)$ are smooth on $[a, b]$, that is, they are several times continuously differentiable on $[a, b]$ [10]. Therefore, we can use the composite q_N-point Gauss-Legendre rule with M uniform subdivisions relative to the coefficients $\{v_\ell\}$ and weights $\{w_\ell\}$ in the interval $[-1, 1]$ as

$$\int_a^b K(x_i, y)z(y)\mathrm{d}y \approx \sum_{q=1}^{M}\sum_{k=1}^{q_N} w_k \frac{\Delta h_q}{2} K(x_i, \theta_k^q)z(\theta_k^q), \tag{18}$$

where $\Delta x = \frac{b-a}{M}$ and $\theta_k^q = \frac{\Delta x}{2} v_\ell + (q - \frac{1}{2})\Delta x$.
Based on the use of composite q_N-point Gauss-Legendre quadrature rule using M subintervals relative to the coefficients $\{y_k\}$ and weights $\{w_k\}$ in the interval $[-1, 1]$, a sequence of numerical integral operators $\mathcal{K}_N$ on $C^{2q_N}[a, b]$ is also introduced from the quadrature rule (18) by

$$\mathcal{K}_N u(x) = \frac{\Delta x}{2} \sum_{k=1}^{q_N} w_k \sum_{q=1}^{M} K(x, \theta_k^q)z(\theta_k^q), \quad N \geq 1, \tag{19}$$

where $\Delta x = \frac{b-a}{M}$ and $\tau_\ell^q = \frac{\Delta x}{2} v_\ell + (q - \frac{1}{2})\Delta x$.
It should be mentioned that $\{\mathcal{K}_N\}$ is a collectively compact set and converges pointwise [23, 36], moreover for every $u \in C^{(2q_N)}[a, b]$ and $K \in C^{(2q_N)}([a, b] \times [a, b])$, we have [23]

$$\|\mathcal{K}u - \mathcal{K}_N u\|_\infty \leq \frac{C_N}{M^{2q_N}} \sup_{x\in[a,b]} |u^{(2q_N)}(x)|. \tag{20}$$

We assume that $\mathcal{K}_N,\ N \geq 1$ on $C[a, b]$ for approximating $\mathcal{K}$ satisfy the following hypotheses [9, 11]:
H1. $\mathcal{K}$ and $\mathcal{K}_N,\ N \geq 1$, are completely continuous nonlinear operators on $C[a, b]$.
H2. $\mathcal{K}_N,\ N \geq 1$ is a collectively compact family on $C[a, b]$, i.e., for every bounded set $B \subset C[a, b]$, the closure of the set $\cup_{N=1}^{\infty} \mathcal{K}_N(B)$ is compact in $C[a, b]$.
H3. $\mathcal{K}_N$ is pointwise convergent to $\mathcal{K}$ on $C[a, b]$, i.e, $\mathcal{K}_N(u) \to \mathcal{K}(u),\ u \in C[a, b]$.
H4. At each point of $C[a, b]$, $\{\mathcal{K}_N\}$ is an equicontinuous family.
H5. $\mathcal{K}$ and $\mathcal{K}_N,\ N \geq 1$ are twice Frechet differentiable on the ball $B(u_0, r)$ and moreover

$$\|\mathcal{K}_N''\| \leq \alpha < \infty, \quad N \geq 1, \quad u \in B(u_0, r). \tag{21}$$

Utilizing the numerical integration scheme (18) in the system (13) yields the nonlinear system of algebraic equations

$$\sum_{k=1}^{N} \hat{z}_k \phi(|x_i - x_k|) = \Psi\left(x_i, f(x_i) + \lambda \sum_{k=1}^{N} \hat{z}_k \sum_{q=1}^{M}\sum_{k=1}^{q_N} w_k \frac{\Delta h_q}{2} K(x_i, \theta_k^q)z(\theta_k^q)\right), \quad i = 1, ..., N, \tag{22}$$

for the unknowns $\{\hat{z}_1, ..., \hat{z}_N\}$. The solution of this system eventually leads to the following numerical solution which can be approximated $z(x)$ as:

$$\hat{z}_N(x) = \sum_{j=1}^{N} \hat{z}_j \phi(|x - x_j|), \quad a \leq x \leq b. \tag{23}$$

We can represent the final systems (22) in the abstract form as

$$\hat{z}_N = \mathcal{R}\mathcal{P}_N(f + \lambda\mathcal{K}_N\hat{z}_N). \tag{24}$$

Finally, we find the numerical solution of the integral equation (1) by

$$\begin{aligned}\hat{u}_N(x) &= f(x) + \lambda\frac{\Delta x}{2}\sum_{k=1}^{q_N} w_k \sum_{q=1}^{M} K(x,\theta_k^q)\hat{z}_N(\theta_k^q)\\ &= f(x) + \lambda\frac{\Delta x}{2}\sum_{k=1}^{q_N} w_k \sum_{q=1}^{M} K(x,\theta_k^q)\sum_{j=1}^{N}\bar{c}_j\phi(|\theta_k^q - x_j|).\end{aligned} \tag{25}$$

In other words, the solution of proposed scheme in the current paper is gotten by

$$\hat{u}_N = f + \lambda\mathcal{K}_N z_N.$$

3. Error estimate

This section describes the error estimate and the convergence rate of the new scheme. We first present the error estimate of RBFs interpolation in terms of the fill distance parameter which mostly follows from [15, 55]. All strictly positive definite functions give rise to reproducing kernels with respect to some Hilbert space which are named native Hilbert spaces.

Definition 3.1. *[55] Suppose $\Phi \in C(\mathbb{R}^d) \cap L^1(\mathbb{R}^d)$ is a real-valued strictly positive definite function. Then the real native Hilbert space respect to reproducing kernel $\Phi(\cdot - \cdot)$ is*

$$\aleph_\Phi(\mathbb{R}^d) = \{f \in C(\mathbb{R}^d) \cap L^2(\mathbb{R}^d) : \frac{\hat{f}}{\sqrt{\hat{\Phi}}} \in L^2(\mathbb{R}^d)\}, \tag{26}$$

with inner product

$$< f, g >_{\aleph_\Phi(\mathbb{R}^d)} = \frac{1}{\sqrt{2\pi}} < \frac{\hat{f}}{\sqrt{\hat{\Phi}}}, \frac{\hat{g}}{\sqrt{\hat{\Phi}}} >_{L^2(\mathbb{R}^d)} = \frac{1}{\sqrt{2\pi}}\int_{\mathbb{R}^d}\frac{\hat{f}(w)\overline{\hat{g}(w)}}{\sqrt{\hat{\Phi}}}\mathrm{d}w, \tag{27}$$

where $\hat{f}$ denotes Fourier transform of f. Furthermore, every $f \in \aleph_\Phi(\mathbb{R}^d)$ has the representation

$$f(x) = \frac{1}{\sqrt{2\pi}}\int_{\mathbb{R}^d}\hat{f}(w)e^{ixw}\mathrm{d}w.$$

From Definition 3.1, we concluded that the native spaces can be regarded as an extension of the standard Sobolev spaces. In other words, if the Fourier transform of strictly positive definite function Φ decays only algebraically, then the function Φ has a corresponding Sobolev space as its native space [25, 55].
We now present some definitions [15, 55] that are important to measure the quality of data points and to estimate the error of RBF interpolation method.

Definition 3.2. *The fill distance of a set of points $X = \{x_1, ..., x_N\} \subseteq [a, b]$ for a bounded domain D is defined by*

$$h_X = \sup_{a\le x\le b}\min_{0\le j\le N}\|x - x_j\|_2.$$

Definition 3.3. *The separation distance of $X = \{x_1, ..., x_N\}$ is defined by*

$$q_X = \frac{1}{2}\min_{i\neq j}\|x_i - x_j\|_2.$$

The set X is said to be quasi-uniform with respect to a constant $c > 0$ if $q_X \le h_X \le cq_X$ [25].

The collocation operator $\mathcal{P}_N : C[a,b] \to C_N[a,b]$ for RBF $\Phi(x) = \phi(|x|)$ is defined by the following linear combination [55]:

$$\mathcal{P}_N u(x) = \sum_{k=1}^{N} c_k \phi(|x - x_k|), \quad a \le x \le b, \tag{28}$$

where where the coefficients $\{c_k\}_{k=1}^{N}$ are determined by the interpolation conditions

$$\mathcal{P}_N u(x_i) = u(x_i), \quad i = 1, ..., N, \tag{29}$$

and

$$C_N[a,b] = \text{span}\{\phi(|x - x_1|), ..., \phi(|x - x_N|)\}.$$

We are ready to represent the convergence theorem for approximating a function $u \in \aleph_\Phi[a,b]$ by the RBF approach [55].

Theorem 3.4. *[55] Assume the interpolant of a function $u \in \aleph_\Phi[a,b]$ is based on the positive definite RBF Φ and the distinct set $X = \{\mathbf{x}_1, ..., \mathbf{x}_N\}$. Then for every $l \in \mathbb{N}$ there exist constants $h_0(l), C_l$ such that*

$$\|u - \mathcal{P}_N u\|_\infty \le C_l h_X^l |u|_{\aleph_\Phi[a,b]}, \tag{30}$$

provided $h_X \le h_0(l)$.

Remark 3.5. *[25] As a conclusion from Theorem 3.4, for the sufficiently small h_X, some positive constant c and $u \in \aleph_\Phi[a,b]$, we list the error bound as follows:*
For Gaussians, we have

$$\|u - \mathcal{P}_N u\|_\infty \le e^{\left(\frac{-c|\log h_{X,D}|}{h_X}\right)} |u|_{\aleph_\Phi[a,b]}. \tag{31}$$

For inverse multiquadrics, we give

$$\|u - \mathcal{P}_N u\|_\infty \le e^{\left(\frac{-c}{h_{X,D}}\right)} |u|_{\aleph_\Phi[a,b]}. \tag{32}$$

Therefore the convergence rates will be arbitrarily high algebraic for infinitely smooth RBFs such as Gaussians and inverse multiquadrics and for RBFs with limited smoothness, the approximation order of the method is limited by the degree of smoothness (see [55], Chapter 11 for details).

Let $Tu = u$ be a fixed point problem on $C[a,b]$ and T be a nonlinear compact operator on $C[a,b]$. Define the approximating operator T_N on $C[a,b]$ to estimate the operator T. The required hypotheses on T and $T_N,\ N \ge 1$ are listed and labeled in the following [9, 11]:
(i) T and $T_N,\ N \ge 1$, are completely continuous nonlinear operators on $C[a,b]$.
(ii) $T_N,\ N \ge 1$ is a collectively compact family on $C[a,b]$.
(iii) T_N is pointwise convergent to T on $C[a,b]$, i.e, $T_N(u) \to T(u),\ u \in C[a,b]$.
(iv) At each point of $C[a,b]$, $\{T_N\}$ is an equicontinuous family.
(v) T and $T_N,\ N \ge 1$ are twice Frechet differential on the ball $B(u_0, r),\ r > 0$ and moreover

$$\|T_N^{''}\| \le \alpha < \infty, \quad N \ge 1,\ u \in B(u_0, r). \tag{33}$$

Lemma 3.6. *Suppose (i)-(v). Let z_0 be a fixed point of T, and assume that 1 is not an eigenvalue of $T'(z_0)$, where $T'(z_0)$ denotes the Frechet derivative of T at z_0. If (v) is satisfied on $B(z_0, r) \subseteq C[a,b]$, then u_0 is a fixed point, of the nonzero index. Moreover, there are $\varepsilon, M > 0$ such that for every $N > M$, T_N has a unique fixed point z_N in $B(u_0, \varepsilon)$. Also, there is a constant $\gamma_2 > 0$ such that*

$$\|z_N - z_0\|_\infty \le \gamma_1 \|Tz_0 - T_N z_0\|_\infty, \quad N \ge M. \tag{34}$$

Consider the nonlinear operators Tz and T_Nz on $C[a,b]$ as follows:

$$Tz \equiv \mathcal{R}(\mathcal{K}z + f),$$

and

$$T_Nz \equiv \mathcal{P}_N\mathcal{R}(\mathcal{K}_Nz + f).$$

Assuming that $\mathcal{K}$ and $\mathcal{K}_N$ satisfies H1-H5, it is shown in [11] that T and T_N also satisfies (i)-(v).
We are ready to consider the convergence theorem about the presented method.

Theorem 3.7. *Suppose that the assumptions of Theorem 3.4 and Lemma 3.6 hold. Let the Hammerstein integral equation (1) have a unique solution $u_0 \in \aleph_\Phi[a,b] \cap C^{2q_N}[a,b]$. Assume that 1 is not an eigenvalue of $\mathcal{R}'(\mathcal{K}z_0 + f)\mathcal{K}'$, where $\mathcal{K}'$ and $\mathcal{R}'$ indicates the Frechet derivatives at z_0. Thus there are $\varepsilon, \bar{M} > 0$ such that the proposed method has a unique solution $\bar{u}_N$ in the ball $B(u_0,\varepsilon)$ for every $N > \bar{M}$. Moreover there exist positive constants $C_1, C_P, C_K, C_N, \gamma_1, h_0$, provided that $h_{X,D} \le h_0$ such that*

$$\|\hat{u}_N - u_0\|_\infty \le C_K|\lambda|\gamma_1 C_l h_X^l |v_0|_{\aleph_\Phi[a,b]} + (C_K\gamma_1 C_P C_1 + 1)\frac{|\lambda|C_N}{M^{2q_N}} \sup_{x\in[a,b]} |z_0^{(2q_N)}(x)|, \tag{35}$$

where $v_0 \equiv \mathcal{R}(\mathcal{K}z_0 + f)$.

Proof. By considering $\hat{u}_N = f + \lambda\mathcal{K}_N\hat{z}_N$, we have

$$\begin{aligned} \|\hat{u}_N - u_0\|_\infty &\le \|(f + \lambda\mathcal{K}_N\hat{z}_N) - (f + \lambda\mathcal{K}z_0)\|_\infty = |\lambda|\|\mathcal{K}_N\hat{z}_N - \mathcal{K}z_0\|_\infty \\ &\le |\lambda|\|\mathcal{K}_N\hat{z}_N - \mathcal{K}_Nz_0\|_\infty + |\lambda|\|\mathcal{K}_Nz_0 - \mathcal{K}z_0\|_\infty, \end{aligned} \tag{36}$$

so it is concluded that

$$\|\hat{u}_N - u_0\|_\infty \le |\lambda|\|\mathcal{K}_N\|\|\hat{z}_N - z_0\|_\infty + |\lambda|\|\mathcal{K}_Nz_0 - \mathcal{K}z_0\|_\infty. \tag{37}$$

Since the family $\mathcal{K}_N$ is the pointwise convergence to $\mathcal{K}$, there exists a constant $M_2 > 0$ such that for every $N > M_2$ we have $\|\mathcal{K}_Nz_0 - \mathcal{K}z_0\| < \varepsilon$ and from the principle of uniform boundedness [10], it can be supposed that $\|\mathcal{K}_N\| \le C_K$. Therefore

$$\|\hat{u}_N - u_0\|_\infty \le |\lambda|C_K\|\hat{z}_N - z_0\|_\infty + |\lambda|\|\mathcal{K}_Nz_0 - \mathcal{K}z_0\|_\infty. \tag{38}$$

Since 1 is not an eigenvalue of $T' \equiv \mathcal{R}'(\mathcal{K}z_0 + f)\mathcal{K}'$, this can be immediately obtained from Lemma 3.6 that there exists a unique solution $z_N \in B(z_0,\varepsilon)$ (i.e., there is a constant $M_1 > 0$ such that for every $N > M_1$ we have $\|\hat{z}_N - z_0\|_\infty < \varepsilon$), such that

$$\|\hat{z}_N - z_0\|_\infty \le \gamma_1\|Tz_0 - T_Nz_0\|_\infty = \gamma_1\|\mathcal{R}(\mathcal{K}z_0 + f) - \mathcal{P}_N\mathcal{R}(\mathcal{K}_Nz_0 + f)\|_\infty.$$

On the other hand, we have

$$\begin{aligned} \|\hat{z}_N - z_0\|_\infty &\le \gamma_1\|\mathcal{R}(\mathcal{K}z_0 + f) - \mathcal{P}_N\mathcal{R}(\mathcal{K}z_0 + f)\|_\infty + \gamma_1\|\mathcal{P}_N\mathcal{R}(\mathcal{K}z_0 + f) - \mathcal{P}_N\mathcal{R}(\mathcal{K}_Nz_0 + f)\|_\infty \\ &\le \gamma_1\|v_0 - \mathcal{P}_Nv_0\|_\infty + \gamma_1\|\mathcal{P}_N\|\|\mathcal{R}(\mathcal{K}z_0 + f) - \mathcal{R}(\mathcal{K}_Nz_0 + f)\|_\infty, \end{aligned}$$

where $v_0 \equiv \mathcal{R}(\mathcal{K}z_0 + f)$. From the principle of the uniform boundedness (see [10], Theorem A.3 in the Appendix), we conclude that

$$C_P = \sup_{N\in\mathbb{N}} \|\mathcal{P}_N\| < \infty. \tag{39}$$

Also, from the assumption (A1) on the Fredholm-Hammerstein integral equation (1), we have

$$\|\mathcal{R}(\mathcal{K}z_0 + f) - \mathcal{R}(\mathcal{K}_Nz_0 + f)\|_\infty \le C_1\|\mathcal{K}z_0 - \mathcal{K}_Nz_0\|_\infty. \tag{40}$$

Therefore, using (39) and (40) results that

$$\|\hat{z}_N - z_0\|_\infty \le \gamma_1\|v_0 - \mathcal{P}_Nv_0\|_\infty + \gamma_1C_PC_1\|\mathcal{K}z_0 - \mathcal{K}_Nz_0\|_\infty. \tag{41}$$

By substituting (41) in (38), we obtain

$$\|\hat{u}_N - u_0\|_\infty \leq C_K\gamma_1\|v_0 - \mathcal{P}_N v_0\|_\infty + (C_K\gamma_1 C_P C_1 + 1)\|\mathcal{K}z_0 - \mathcal{K}_N z_0\|_\infty.$$

Choosing $\hat{M} = \max\{M_1, M_2\}$, we deduce that $\hat{u}_N$, for $N > M$, within $B(u_0, \hat{\varepsilon})$, is the unique solution of the proposed method, because

$$\|\hat{u}_N - u_0\|_\infty \leq (C_2\varepsilon + \varepsilon) = \hat{\varepsilon}. \tag{42}$$

It is seen $z_0(x) = \Phi(x, u_0(x))$ in $\aleph_\Phi[a,b] \cap C^{2q_N}[a,b]$, because Φ is a well-behaved function on $[a,b] \times \mathbb{R}$ and $u_0 \in \aleph_\Phi[a,b] \cap C^{2q_N}[a,b]$. Finally using Theorem 3.4 and the error bound (20), we have

$$\|\hat{u}_N - u_0\|_\infty \leq C_K|\lambda|\gamma_1 C_l h_X^l |v_0|_{\aleph_\Phi[a,b]} + (C_K\gamma_1 C_P C_1 + 1)\frac{|\lambda|C_N}{M^{2q_N}} \sup_{x\in[a,b]} |z_0^{(2q_N)}(x)|.$$

Since, $h_{X,D} \to 0$ as $N \to \infty$ (justified by the quasi-uniform condition on X), yields $\hat{u}_N \to u_0$. This completes the proof. □

4. Numerical examples

To study the accuracy and efficiency of the new method, we have solved four test problems involving Hammerstein integral equations. The Gaussians (GAs) and the inverse multiquadrics (IMQs) are applied for solving these types of integral equations. In computations, we put $c = 0.11\times\sqrt{N}$ for GAs and $c = \frac{3}{\sqrt{N}}$ for IMQs based on the discussion on selection shape parameter in [2, 26]. We utilize 10-points composite Gauss-Legendre quadrature formula with subdivisions $M = 10$ to compute integrals in the scheme. Furthermore, the numerical results are compared with the method presented in [36] based on the use of Legendre wavelets $\psi_{nm}(x) = \psi(k, m, x)$, in which $k = 2, 3, ...$ and $m = 0, 1, ..., M-1$. Wavelets as localized functions are useful for solving nonlinear integral equations [1, 36]. We have obtained the following conclusions by this comparison:

✓ The Legendre wavelet method leads to a larger system with $n = M2^{k-1}$ unknowns instead of the proposed method.

✓ The obtained results of the presented scheme are better than the results given by the Legendre wavelet method.

✓ The proposed method has a simple algorithm based on some random nodes over the $[a, b]$ in compared with the Legendre wavelet method.

✓ The convergence rates of the proposed method are higher than the convergence rates of the Legendre wavelet method.

We have measured the accuracy of presented technique by the maximum error $\|e_N\|_\infty$ and the mean error $\|e_N\|_2$ which can be defined as follows:

$$\|e_k\|_\infty = \max_{x\in[a,b]}\{|u_{ex}(x) - \hat{u}_{N,M}(x)|\}, \quad \|e_k\|_2 = \left(\int_a^b |u_{ex}(x) - \hat{u}_{N,M}(x)|^2 \mathrm{d}x\right)^{\frac{1}{2}},$$

where the exact solution $u_{ex}(x)$ is estimated by the numerical solution $\hat{u}_{N,M}(x)$ obtained by the current paper. The convergence rates of the presented scheme have been also reported by

$$Ratio = \frac{\ln(\|e_N\|_\infty) - \ln(\|e_{N'}\|_\infty)}{\ln(N') - \ln(N)}.$$

We have written all routines in "Maple" software with the "Digits" 20 (Digits environment variable controls the number of digits in Maple) and a Laptop with 2.10 GHz of Core 2 CPU and 4 GB of RAM has been used to run these. To solve the final nonlinear system of algebraic equations the "Fsolve" command has been employed based on the use of floating-point arithmetic. In this command, the selection of initial guesses is very important for converge issue. Here, for $N \leq 6$, we choose the zero vector of length N as initial

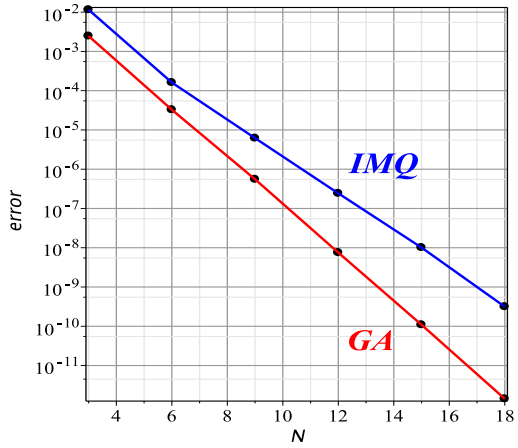

Figure 1: Absolute error distributions of Example 4.1

Table 1: Some numerical results for Example 4.1

N	*GA*			*IMQ*			Legendre wavelet		
	$\|e_N\|_2$	$\|e_N\|_\infty$	Ratio	$\|e_N\|_2$	$\|e_N\|_\infty$	Ratio	n	$\|e_N\|_2$	$\|e_N\|_\infty$
3	1.65×10^{-3}	2.46×10^{-3}	–	8.36×10^{-3}	1.15×10^{-2}	–	3	4.86×10^{-3}	1.12×10^{-2}
6	1.16×10^{-5}	3.27×10^{-5}	4.71	5.41×10^{-5}	1.61×10^{-4}	6.15	6	1.34×10^{-3}	3.08×10^{-3}
9	1.87×10^{-7}	5.53×10^{-7}	8.68	1.64×10^{-6}	6.18×10^{-6}	8.05	12	2.14×10^{-4}	4.93×10^{-4}
12	2.51×10^{-9}	7.52×10^{-9}	14.49	7.92×10^{-8}	2.43×10^{-7}	11.24	24	9.95×10^{-6}	2.29×10^{-5}
15	3.64×10^{-11}	1.09×10^{-11}	17.53	5.31×10^{-9}	1.01×10^{-8}	14.28	48	3.56×10^{-6}	8.20×10^{-6}
18	4.15×10^{-13}	1.42×10^{-12}	22.37	8.05×10^{-11}	3.15×10^{-10}	19.03	96	5.08×10^{-7}	1.15×10^{-6}

guesses [2]. Also, to select the initial guesses for $N > 6$, we apply the obtained solutions corresponding to the nodal points whose number is less than N. In other words, we assume that $\hat{u}_\tau$ is the approximate solution which is obtained by the presented method for $\tau < N$, then consider the following linear system of algebraic equations

$$\sum_{k=1}^{N} c_k^{(0)} \phi(|x_i - x_k|) = \hat{u}_\tau(x_i), \quad i = 1, ..., N, \tag{43}$$

The initial value may be chosen as the solution of system (43), i.e, $\hat{u}^{(0)} = [c_1^{(0)}, ..., c_N^{(0)}]^t$. Next, we increase the value of τ until a satisfactory convergence is achieved [2].

Example 4.1. Consider the following Fredholm-Hammerstein integral equation of the second kind:

$$u(x) - \int_0^{\ln 3} \frac{\ln(1 + x^2 + y^2)}{x^2 y + \pi} \frac{\sinh(u(y) + y)}{y^2 \cosh(y) + 1} \, dy = f(x), \quad 0 \le x \le \ln 3, \tag{44}$$

where the function $f(x)$ has been so chosen that the exact solution is

$$u_{ex}(x) = \frac{x}{\sqrt{1 + x^2}}.$$

The traditional methods take difficulty for numerically solving this problem, but using some nodes scattered over the interval $[0, \ln 3]$, this problem could be solved using the meshless method proposed in this paper.

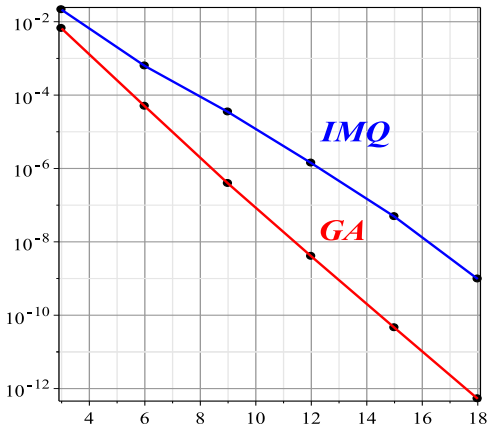

Figure 2: Absolute error distributions of Example 4.2

Table 2: Some numerical results for Example 4.2

N	*GA*			*IMQ*			Legendre wavelet		
	$\|\|e_N\|\|_2$	$\|\|e_N\|\|_\infty$	Ratio	$\|\|e_N\|\|_2$	$\|\|e_N\|\|_\infty$	Ratio	n	$\|\|e_N\|\|_2$	$\|\|e_N\|\|_\infty$
3	3.85×10^{-3}	6.55×10^{-3}	–	1.34×10^{-2}	2.12×10^{-2}	–	3	1.84×10^{-3}	4.18×10^{-3}
6	1.90×10^{-5}	4.95×10^{-5}	5.33	2.08×10^{-4}	6.22×10^{-4}	5.08	6	2.87×10^{-4}	6.62×10^{-4}
9	1.06×10^{-7}	3.89×10^{-7}	10.30	1.61×10^{-5}	3.46×10^{-5}	7.12	12	1.42×10^{-5}	3.27×10^{-5}
12	9.32×10^{-10}	4.02×10^{-9}	14.35	5.99×10^{-7}	1.40×10^{-6}	11.13	24	3.97×10^{-6}	9.14×10^{-6}
15	8.89×10^{-12}	4.54×10^{-11}	18.59	2.31×10^{-8}	4.85×10^{-8}	15.08	48	6.39×10^{-7}	1.47×10^{-6}
18	9.70×10^{-14}	5.26×10^{-13}	22.95	4.82×10^{-10}	9.69×10^{-10}	21.45	96	6.12×10^{-8}	1.34×10^{-7}

Table 1 shows results in terms of $\|e\|_2$, $\|e\|_\infty$ and the rate of convergence for different numbers of N utilizing GAs and IMQs. Also, the results are compared with the method in [36] based on the use of Legendre wavelets for solving Hammerstein integral equations. As we expected from Theorem 3.7, the results converge to the exact values of $O(h^l_{X,D})$ where the used RBF is $2l$ times continuously differentiable [55]. Since GAs and IMQs are several times continuously differentiable, the convergence rate of method is arbitrarily high. We compared the obtained errors for different numbers of N in Figure 1.

Example 4.2. In this example, we solve the integral equation

$$u(x) - \int_0^e \frac{e^{x+y+3}}{x^2+1}\sqrt{\frac{u^2(y)+1}{y^2+\pi}}\,\mathrm{d}y = f(x), \quad 0 \le x \le e, \tag{45}$$

where the function $f(x)$ has been so chosen that the exact solution is

$$u_{ex}(x) = (x^2+1)\ln(1+x).$$

Table 2 shows results in terms of $\|e\|_2$, $\|e\|_\infty$ and the rate of convergence for different numbers of N utilizing GAs and IMQs. To compare the presented method, we also solve the integral equation utilizing the Legendre wavelet method [36] and the numerical results are given in this table. By increasing the number of nodes, the numerical results converge to the exact values with high order and these confirm the theoretical error estimates. We also compared the obtained errors for different numbers of N in Figure 2.

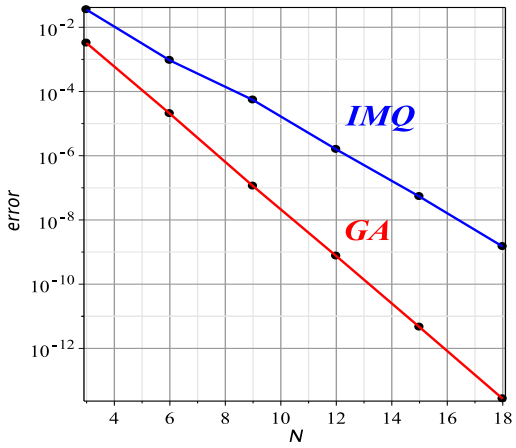

Figure 3: Absolute error distributions of Example 4.3

Example 4.3. Consider the following second-kind Hammerstein integral equation:

$$u(x) - \int_0^{\frac{\pi}{2}} \frac{\sqrt{x^2+y}}{x^2+xy+\pi} \ln\left(1+\frac{u(y)}{e^y+1}\right) dy = f(x), \quad 0 \le x \le \frac{\pi}{2}, \tag{46}$$

where the function $f(x)$ has been so chosen that the exact solution is

$$u_{ex}(x) = \sin(\frac{x}{x+1}).$$

Table 3 shows results in terms of $\|e\|_2$, $\|e\|_\infty$ and the rate of convergence for different numbers of N utilizing GAs and IMQs. Also, the results are compared with the method in [36] based on the use of Legendre wavelets for solving Hammerstein integral equations. It is seen that the obtained numerical results converge to the exact solution by increasing the nodal point selected randomly on $[0, \frac{\pi}{2}]$. Also, it should be noted that from Theorem 3.7, for sufficiently large q_N, the error of the RBF interpolation is dominated over the integration error. Therefore, increasing the number of nodes in numerical integration method has no significant effect on the error. We compared the obtained errors for different numbers of N in Figure 3.

Example 4.4. We consider the following Fredholm-Hammerstein integral equation:

$$u(x) - \int_0^1 \frac{(x+y)^2}{e^{x+y^2+\pi}} \frac{u(y)}{1+u(y)} dy = f(x), \quad 0 \le x \le 1, \tag{47}$$

where the function $f(x)$ has been so chosen that the exact solution is

$$u_{ex}(x) = (x^3+1)e^{\frac{x}{x+1}}.$$

Table 4 shows results in terms of $\|e\|_2$, $\|e\|_\infty$ and the rate of convergence for different numbers of N utilizing GAs and IMQs. To compare the presented method, we also solve the integral equation utilizing the Legendre wavelet method [36] and the numerical results are given in this table. The results obtained in this example demonstrate that the method can be easily used for various kinds of Hammerstein integral equations. We compared the obtained errors for different numbers of N in Figure 4.

Table 3: Some numerical results for Example 4.3

N	*GA*			*IMQ*			Legendre wavelet		
	$\|e_N\|_2$	$\|e_N\|_\infty$	Ratio	$\|e_N\|_2$	$\|e_N\|_\infty$	Ratio	n	$\|e_N\|_2$	$\|e_N\|_\infty$
3	1.89×10^{-3}	3.21×10^{-3}	–	2.30×10^{-2}	3.51×10^{-2}	–	3	2.33×10^{-3}	5.98×10^{-3}
6	7.99×10^{-6}	2.04×10^{-5}	5.52	3.11×10^{-4}	9.30×10^{-4}	5.23	36	3.56×10^{-4}	9.17×10^{-4}
9	3.15×10^{-8}	1.13×10^{-7}	11.05	2.57×10^{-5}	5.42×10^{-5}	7.01	12	4.76×10^{-5}	1.24×10^{-4}
12	1.79×10^{-10}	7.50×10^{-10}	0.866	8.61×10^{-7}	1.57×10^{-6}	12.31	24	6.31×10^{-6}	1.64×10^{-5}
15	9.23×10^{-13}	4.59×10^{-12}	0.744	1.17×10^{-8}	5.33×10^{-8}	15.17	48	9.22×10^{-7}	2.41×10^{-6}
18	5.15×10^{-15}	2.69×10^{-14}	0.707	8.59×10^{-10}	1.48×10^{-9}	19.64	96	1.14×10^{-7}	2.87×10^{-7}

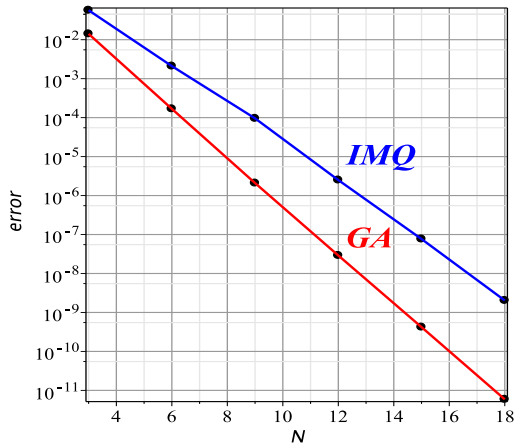

Figure 4: Absolute error distributions of Example 4.4

Table 4: Some numerical results for Example 4.4

N	*GA*			*IMQ*			Legendre wavelet		
	$\|e_N\|_2$	$\|e_N\|_\infty$	Ratio	$\|e_N\|_2$	$\|e_N\|_\infty$	Ratio	n	$\|e_N\|_2$	$\|e_N\|_\infty$
3	8.23×10^{-3}	1.41×10^{-2}	–	3.42×10^{-2}	5.69×10^{-2}	–	3	2.02×10^{-2}	4.87×10^{-2}
6	6.21×10^{-4}	1.68×10^{-4}	4.83	7.56×10^{-4}	2.10×10^{-3}	3.59	6	3.59×10^{-3}	7.79×10^{-3}
9	5.62×10^{-7}	2.09×10^{-6}	9.33	4.01×10^{-5}	9.56×10^{-5}	6.57	12	5.48×10^{-4}	1.18×10^{-3}
12	6.71×10^{-9}	2.90×10^{-8}	13.42	9.81×10^{-7}	2.51×10^{-6}	11.44	24	7.53×10^{-5}	1.62×10^{-4}
15	8.09×10^{-11}	4.21×10^{-10}	17.56	2.39×10^{-8}	7.66×10^{-8}	14.45	48	9.93×10^{-6}	2.14×10^{-5}
18	1.12×10^{-12}	5.89×10^{-12}	21.97	8.17×10^{-10}	2.03×10^{-9}	18.69	96	1.24×10^{-6}	2.57×10^{-6}

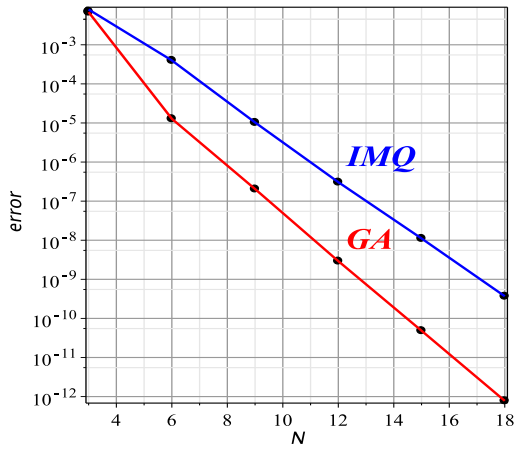

Figure 5: Absolute error distributions of Example 4.5

Table 5: Some numerical results for Example 4.5

N	GA			IMQ			Legendre wavelet		
	$\|e_N\|_2$	$\|e_N\|_\infty$	Ratio	$\|e_N\|_2$	$\|e_N\|_\infty$	Ratio	n	$\|e_N\|_2$	$\|e_N\|_\infty$
3	4.42×10^{-3}	6.84×10^{-3}	–	3.87×10^{-3}	7.19×10^{-3}	–	3	9.86×10^{-3}	2.47×10^{-2}
6	6.01×10^{-6}	1.28×10^{-5}	6.85	1.80×10^{-4}	3.98×10^{-4}	4.17	6	1.91×10^{-3}	4.73×10^{-3}
9	6.57×10^{-8}	2.04×10^{-7}	8.80	4.51×10^{-5}	1.03×10^{-5}	9.01	12	2.78×10^{-4}	6.98×10^{-4}
12	6.97×10^{-10}	2.92×10^{-9}	13.33	1.13×10^{-7}	3.06×10^{-7}	12.23	24	4.03×10^{-5}	9.81×10^{-5}
15	8.82×10^{-12}	4.84×10^{-11}	17.01	7.23×10^{-9}	1.12×10^{-8}	14.86	48	4.97×10^{-6}	1.21×10^{-5}
18	1.26×10^{-13}	7.79×10^{-13}	21.26	8.99×10^{-11}	3.69×10^{-10}	18.65	96	6.48×10^{-7}	1.57×10^{-6}

Example 4.5. As the final example, let

$$u(x) - \int_0^{sih(1)} \frac{\sin(xy+1)}{(xy+1)^2} \frac{e^{y+u(y)}}{y^2+1} \, dy = f(x), \quad 0 \le x \le sih(1), \tag{48}$$

where the function $f(x)$ has been so chosen that the exact solution is

$$u_{ex}(x) = \frac{(x^2+1)}{x+\pi^2}.$$

Table 5 shows results in terms of $\|e\|_2$, $\|e\|_\infty$ and the rate of convergence for different numbers of N utilizing GAs and IMQs. Also, the results are compared with the method in [36] based on the use of Legendre wavelets for solving Hammerstein integral equations. As we can see from Theorem 3.7, the results gradually converge to the exact values as $N \to \infty$ of order h_X^l which results converge to the exact values of arbitrarily high, because the used RBFs in this paper are smooth. We compared the obtained errors for different numbers of N in Figure 5.

5. Conclusion

The main purpose of this article is to investigate a computational scheme for solving Fredholm-Hammerstein integral equations of the second kind. The method estimates the solution by the collocation method based on the use of RBF approach. The discrete collocation method for solving integral equations

results from the numerical integration of all integrals appeared in the method. The proposed scheme applies a accurate quadrature formula via the Gauss-Legendre integration rule to compute integrals in the scheme. Since the proposed method does not require any background mesh, we can call it as the meshless discrete collocation method. We also obtain the error bound and the convergence rate of the presented method. Finally, numerical examples are included to show the validity and efficiency of the new technique and confirm the theoretical error estimates.

Acknowledgments

The author is very grateful to the reviewers for their valuable comments and suggestions which have improved the paper.

References

[1] H. Adibi, P. Assari. On the numerical solution of weakly singular Fredholm integral equations of the second kind using Legendre wavelets. J. Vib. Control., 17 (2011) 689–698.
[2] P. Assari, H. Adibi, M. Dehghan. A meshless method for solving nonlinear two-dimensional integral equations of the second kind on non-rectangular domains using radial basis functions with error analysis. J. Comput. Appl. Math., 239 (2013) 72–92.
[3] P. Assari, H. Adibi, M. Dehghan. A meshless discrete Galerkin (MDG) method for the numerical solution of integral equations with logarithmic kernels. J. Comput. Appl. Math., 267 (2014) 160–181.
[4] P. Assari, H. Adibi, M. Dehghan. A meshless method based on the moving least squares (MLS) approximation for the numerical solution of two-dimensional nonlinear integral equations of the second kind on non-rectangular domains. Numer. Algor., 67 (2014) 423–455.
[5] P. Assari, H. Adibi, M. Dehghan. The numerical solution of weakly singular integral equations based on the meshless product integration (MPI) method with error analysis. Appl. Numer. Math., 81 (2014) 76–93.
[6] P. Assari, M. Dehghan. A meshless method for the numerical solution of nonlinear weakly singular integral equations using radial basis functions. Eur. Phys. J. Plus., 132 (2017) 1–23.
[7] P. Assari, M. Dehghan. The numerical solution of two-dimensional logarithmic integral equations on normal domains using radial basis functions with polynomial precision. Eng. Comput., 33 (2017) 853–870.
[8] P. Assari, M. Dehghan. Solving a class of nonlinear boundary integral equations based on the meshless local discrete Galerkin (MLDG) method. Appl. Numer. Math., 123 (2018) 137–158.
[9] K. E. Atkinson. The numerical evaluation of fixed points for completely continuous operators. SIAM J. Numer. Anal., 10 (1973) 799–807.
[10] K. E. Atkinson. The Numerical Solution of Integral Equations of the Second Kind. Cambridge University Press, Cambridge, 1997.
[11] K. E. Atkinson, J. Flores. The discrete collocation method for nonlinear integral equations. IMA J. Numer. Anal., 13 (1993) 195–213.
[12] K.E. Atkinson, F.A. Potra. Projection and iterated projection methods for nonlinear integral equations. SIAM J. Numer. Anal., 24 (1987) 1352–1373.
[13] J. Boersma, E. Danicki. On the solution of an integral equation arising in potential problems for circular and elliptic disks. SIAM J. Appl. Math., 53 (1993) 931–941.
[14] V. Rokhlin, J. Bremer, I. Sammis. Universal quadratures for boundary integral equations on two-dimensional domains with corners. J. Comput. Physics, 229 (2010) 8259–8280.
[15] M. D. Buhmann. Radial Basis Functions: Theory and Implementations. Cambridge University Press, Cambridge, 2003.
[16] P. Dasa, G. Nelakantia, G. Longb. Discrete Legendre spectral projection methods for Fredholm-Hammerstein integral equations. J. Comput. Appl. Math., 278 (2015) 293–305.
[17] M. Dehghan, R. Salehi. The numerical solution of the non-linear integro-differential equations based on the meshless method. J. Comput. Appl. Math., 236 (2012) 2367–2377.
[18] M. Dehghan, A. Shokri. A numerical method for KdV equation using collocation and radial basis functions. Nonlinear Dyn., 50 (2007) 111–120.
[19] M. Dehghan, A. Shokri. A numerical method for solution of the two-dimensional sine-Gordon equation using the radial basis functions. Math. Comput. Simulat., 79 (2008) 700–715.
[20] M. Dehghan, A. Shokri. Numerical solution of the nonlinear Klein-Gordon equation using radial basis functions. J. Comput. Appl. Math., 230 (2009) 400–410.
[21] H. Dobner. Bounds for the solution of hyperbolic problems. Computing., 38 (1987) 209–218.
[22] M. Erfanian, M. Gachpazan, H. Beiglo. Rationalized Haar wavelet bases to approximate solution of nonlinear Fredholm integral equations with error analysis. Appl.Math. Comput., 265 (2015) 304–312.
[23] W. Fang, Y. Wang, Y. Xu. An implementation of fast wavelet Galerkin methods for integral equations of the second kind. J. Sci. Comput., 20 (2004) 277–302.
[24] R. Farengo, Y.C. Lee, P.N. Guzdar. An electromagnetic integral equation: Application to microtearing modes. Phys. Fluids, 26 (1983) 3515–3523.

[25] G. E. Fasshauer. Meshfree methods. In Handbook of Theoretical and Computational Nanotechnology. American Scientific Publishers, 2005.
[26] G. E. Fasshauer, J. G. Zhang. On choosing "optimal" shape parameters for RBF approximation. Numer. Algor., 45 (2007) 345–368.
[27] R. Franke. Scattered data interpolation: Tests of some methods. Math. Comput, 38 (1982) 181–200.
[28] L. Grammonta, P. B. Vasconcelos, M. Ahuesa. A modified iterated projection method adapted to a nonlinear integral equation. Appl. Math. Comput., 276 (2016) 432–441.
[29] J. Guo, J. H. Jung. Radial Basis Function ENO and WENO Finite Difference Methods Based on the Optimization of Shape Parameters. J. Sci. Comput., 70 (2017) 551-575.
[30] J. Guo, J. H. Jung. A RBF-WENO finite volume method for hyperbolic conservation laws with the monotone polynomial interpolation method. Numer. Math., 122 (2017) 27–50.
[31] H. Guoqiang, W. Jiong. Extrapolation of Nystrom solution for two dimensional nonlinear Fredholm integral equations. J. Comput. Appl. Math., 134 (2001) 259–268.
[32] R. L. Hardy. Hardy, multiquadric equations of topography and other irregular surfaces. J. Geophys. Res., 176 (2006) 1905–1915.
[33] Y. C. Hon, X. Z. Mao. An efficient numerical scheme for Burgers' equation. Appl. Math. Comput., 95 (1998) 37–50.
[34] Y. C. Hon, K. F. Cheung, X. Mao, E. J. Kansa. Multiquadric solution for shallow water equations. ASCE J. Hydraul. Eng., 125 (1999) 524–533.
[35] Y. C. Hon, X. Z. Mao. A radial basis function method for solving options pricing model. Financ. Eng., 8 (1999) 31–49.
[36] H. Kaneko, Y. Xu. Gauss-type quadratures for weakly singular integrals and their application to Fredholm integral equations of the second kind. Math. Comp., 62 (1994) 739–753.
[37] H. Kaneko, Y. Xu. Superconvergence of the iterated Galerkin methods for Hammerstein equations. SIAM J. Numer. Anal., 33 (1996) 1048–1064.
[38] S. Kumar. A discrete collocation-type method for Hammerstein equations. SIAM J. Numer. Anal., 25 (1998) 328–341.
[39] S. Kumar, I. H. Sloan. A new collocation type method for Hammerstein integral equations. Math. Comput., 48 (1987) 585–593.
[40] U. Lepik. Solving integral and differential equations by the aid of non-uniform Haar wavelets. Appl. Math. Comput., 198 (2008) 326–332.
[41] X. Li, J. Zhu. A Galerkin boundary node method and its convergence analysis. J. Comput. Appl. Math., 230 (2009) 314–328.
[42] A. V. Manzhirov. On a method of solving two-dimensional integral equations of axisymmetric contact problems for bodies with complex rheology. J. Appl. Math. Mech., 49 (1985) 777–782.
[43] J. Meinguet. Multivariate interpolation at arbitrary points made simple. Z. Angew. Math. Phys., 30 (1979) 292–304.
[44] M. V. Mirkin, A. J. Bard. Multidimensional integral equations. part 1. a new approach to solving microelectrode diffusion problems. J. Electroad. Chem., 323 (1992) 1–27.
[45] D. Mirzaei, M. Dehghan. A meshless based method for solution of integral equations. Appl. Numer. Math., 60 (2010) 245–262.
[46] Y. Ordokhani. Solution of FredholmHammerstein integral equations with Walsh-hybrid functions. Int. Math. Forum., 4 (2009) 969–976.
[47] I. J. Schoenberg. Metric spaces and completely monotone functions. Ann. Math., 39 (1938) 811–841.
[48] A. Shokri, M. Dehghan. A not-a-knot meshless method using radial basis functions and predictor-corrector scheme to the numerical solution of improved boussinesq equation. Comput. Phys. Comm., 181 (2010) 1990–2000.
[49] M. Tatari, M. Dehghan. On the solution of the non-local parabolic partial differential equations via radial basis functions. Appl. Math. Model., 33 (2009) 1729–1738.
[50] G. Wahba. Convergence rate of "thin plate" smoothing splines when the data are noisy (preliminary report). Springer Lecture Notes in Math., 757 (1979) 233–245.
[51] L. Wang, Z. Wang, Z. Qian. A meshfree method for inverse wave propagation using collocation and radial basis functions. Comput. Methods Appl. Mech. Eng., 322 (2017) 311–350.
[52] L. Wang. Radial basis functions methods for boundary value problems: Performance comparison. Eng. Anal. Bound. Elem., 84 (2017) 191–205.
[53] L. Wang, J. S. Chen, H. Y. Hu. Subdomain radial basis collocation method for fracture mechanics. Int. J. Numer. Methods Eng., 83 (2010) 851–876.
[54] A.M. Wazwaz. Linear and Nonlinear Integral equations: Methods and Applications. Higher Education Press and Springer Verlag, Heidelberg, 2011.
[55] H. Wendland. Scattered Data Approximation. Cambridge University Press, New York, 2005.
[56] M. Zerroukat, H. Power, C.S. Chen. A numerical method for heat transfer problems using collocation and radial basis functions. Internat. J. Numer. Methods Eng., 42 (1998) 1263–1278.